Presented at the 24th European PV Solar Energy Conference and Exhibition, 21-25 September 2009, Hamburg, Germany

OVERVIEW ON CRYSTALLINE SILICON SOLAR CELLS USING PECVD REAR PASSIVATION AND LASER-FIRED CONTACTS

Marc Hofmann, Pierre Saint-Cast, Dominik Suwito, Johannes Seiffe, Christian Schmidt[1], Stephan Kambor[2], Luca Gautero, Norbert Kohn, Jan-Frederik Nekarda, Antonio Leimenstoll, Dirk Wagenmann, Denis Erath, Jan Catoir, Winfried Wolke, Stefan Janz, Daniel Biro, Andreas Grohe, Jochen Rentsch, Stefan W. Glunz and Ralf Preu

Fraunhofer Institute for Solar Energy Systems (ISE)
Heidenhofstrasse 2, D-79110 Freiburg, Germany
phone: +49 761-4588-5614; fax: +49 761-4588-9250
email: marc.hofmann@ise.fraunhofer.de

ABSTRACT: Solar cells of "classic" external contact structure with front and rear contacts applying a passivated and locally contacted rear are presented in this paper. A variety of rear surface passivation schemes deposited by PECVD are discussed and compared using illuminated I-V, reflection and internal quantum efficiency measurements with fixed and variable bias light intensities. All cells presented were contacted on the rear by laser-firing. It is shown that amorphous hydrogenated silicon (a-Si) stacked with amorphous hydrogenated silicon oxide (SiO_x) is reaching a comparable level of rear surface passivation as thermally grown silicon dioxide (SiO_2) and that the bias-light dependence of such cells is lower than that of SiO_2 or amorphous hydrogenated silicon nitride (SiN_x) stacked with SiO_x passivated cells. Additionally, firing stable stacks of SiO_x, SiN_x and SiO_x are compared to SiC_x and the above mentioned layer systems.
Keywords: Passivation, PECVD, high-efficiency

1 INTRODUCTION

The major goal of research in crystalline silicon solar cell technology is to reduce the price per wattpeak. Therefore, new cell designs and new production processes have been developed in the past. Widely used in laboratories around the world is the PERC (passivated emitter and rear cell) concept [1]. Due to its relatively high production costs, this cell concept has not made the step into solar cell mass production yet.

By the use of the Laser-Fired Contacts (LFC) approach [2], an economically feasible technology for mass production of the local rear contacts of PERC cells has been introduced.

In the next step, rear side surface passivation schemes need to be adapted to the LFC process and to the industrial production environment. As thermally grown silicon dioxide (SiO_2) layers are manufactured by a long-time and energy-intensive high temperature process, they are not the first choice for mass production, although they possibly provide a very good and thermally stable passivation.

Plasma-enhanced chemical vapour deposited (PECVD) layers can alternatively be used for the passivation of the rear surface. This paper compares the results of the different PECVD approaches. Solar cell IV parameters and spectral response behaviour will be discussed in the paper as well as the potential to be implemented in a industrial production environment.

PERC type cells are favoured for the next generation of industrially produced cells due to relatively little changes in the solar cell structure and the production equipment compared to the standard cell manufacturing today. Furthermore, it allows for a standard or only slightly modified module manufacturing. Another great advantage is the possibility to produce cells with very low or no bowing because no full-area rear contact between metal and Si is formed. Hence, also very thin cells (<130 µm) can meaningfully be produced.

In this publication, PECVD layers of amorphous hydrogenated silicon (a-Si:H, in short: a-Si), amorphous hydrogenated silicon nitride (a-SiN_x:H, in short: SiN_x) , both stacked with hydrogenated amorphous silicon oxide (a-SiO_x:H, in short: SiO_x), amorphous hydrogenated silicon carbide (a-SiC_x:H, in short: SiC_x) and triple stacks of SiO_x, SiN_x and SiO_x are compared with thermally grown silicon dioxide (SiO_2) and screen-printed and fired Al-BSF.

2 SOLAR CELL STRUCTURE AND MANUFACTURING

The PERC-type cells were prepared at Fraunhofer ISE using high-quality float zone silicon material. A saw damage etch has been performed already at the wafer manufacturer site. Additionally, the wafers' surfaces were shiny etched. Hence, the process starts with a wet chemical surface clean and subsequently we thermally oxidise the surfaces at ~1000 °C resulting in a thick SiO2 layer on both surfaces. A lacquer protection is deposited on the rear and partly on the front leaving open windows on the front. The oxide on the front windows is removed in a HF bath. After removing the lacquer, random pyramids are etched wet chemically in a KOH solution. The oxide on the rear serves as a protection layer during this step. Hence, pyramidal structures are formed only at the front. After a wet chemical surface cleaning the phosphorus diffusion step is performed resulting in an emitter formation only at the front. The oxide at the rear serves as a protection layer during this step as well. Subsequently, a second oxidation is performed after a wet chemical surface cleaning creating the anti-reflection coating (ARC) at the front, driving in the emitter and thickening the rear oxide. Optionally, the oxide on the

[1] now with Oerlikon Solar AG, Hauptstrasse 1a, 9477 Trübbach, Switzerland
[2] now with Roth&Rau AG, An der Baumschule 6-8, 09337 Hohenstein-Ernstthal, Germany

rear can now be removed and replaced by an alternative passivation layer like PECVD layer systems. The next step is the photolithographical local opening of the front oxide to allow the contact formation of the front fingers. Subsequently, a metal stack consisting of Ti, Pd and Ag is evaporated on the front. The lift off of the lacquer removes the parasitic metal between the contact fingers. We evaporate Al on the full rear surface and subsequently use a pulsed laser system to locally melt the Al on the rear and create local rear point contacts through the typically isolating passivating layer system. Electroplating of the front contacts in a Ag bath thickens the front contacts and allows for a reasonable lateral conductivity in the front fingers (sufficient metal finger cross section). A final anneal of the solar cell in forming gas enhances the LFC performance and the oxide passivation quality. The workflow can be found in Figure 1.

This photolithographic clean-room approach is, of course, quite costly and lengthy but allows for excellent solar cell efficiencies. Hence, the performance of rear surface passivation layers can be studied very well.

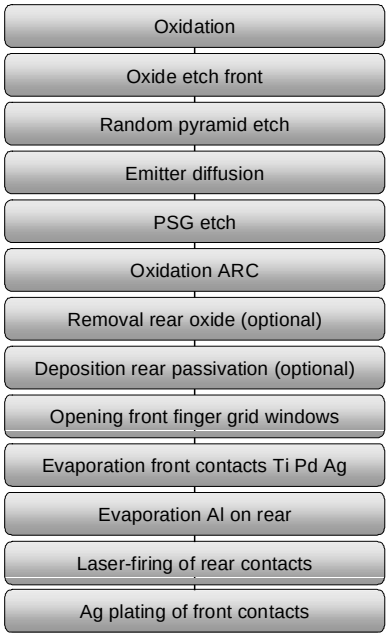

Figure 1: Workflow of the manufacturing of the high-efficiency cells presented in this work.

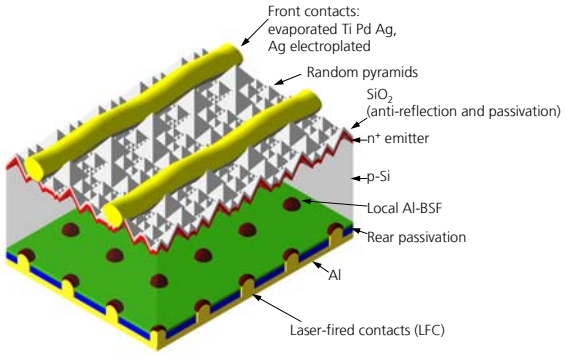

Figure 2: Sketch of the solar cells fabricated in this work.

3 a-Si:H + a-SiO_x:H or a-SiN_x:H REAR PASSIVATION

a-Si has shown an excellent level of rear surface passivation on high-efficiency solar cell structures [3-6]. Especially, when the a-Si is stacked with either PECVD SiO_x [5, 6] or SiN_x [4] of sufficient thickness, the cells perform best due to the improved internal rear reflectivity. Additionally, these stacks improve the thermal stability of the a-Si passivation [7] and provide a protection of the a-Si from the Al layer.

a-Si layers can be deposited at very low temperatures. A deposition temperature of ~100 °C has been demonstrated that leads to excellent passivation if an additional annealing, preferably above 200 °C, is applied [4]. Brendle et al. have shown excellent solar cell results using this very-low-temperature approach reaching an efficiency of 20.5% when applying a stack of a-Si and SiN_x on the rear. Open-circuit voltage V_{OC} and short-circuit current J_{SC} were giving excellent numbers of 670 mV and 39.9 mA/cm2, respectively. Mainly the limited fill factor FF of 76.5% was preventing the cells from being even better.

At Fraunhofer ISE, a stack of a-Si and SiOx was used to passivate the rear of LFC-PERC cells. Here, an efficiency of 21.7% was reached showing excellent results in V_{OC} (677 mV), J_{SC} (39.5 mA/cm2) and FF (81.1%) [5, 6]. When analysing quantum efficiency and reflection curves for this cell using PC1D modelling and applying the equation of Fischer ([8], page 38) and the parametrisation of Kray et al. [9] we extracted the rear passivation quality of the cell to be $S_{eff,\,pass}$=120 cm/s ± 30 cm/s. See the external EQE, internal quantum efficiency IQE, reflection and the fit in Figure 3.

No principal physical problems of rear passivation applying these stacks were found.

The deposition of the a-Si and SiO_x layers were performed in a single-wafer reactor (Multiplex CVD by Surface Technology Systems) [5, 6].

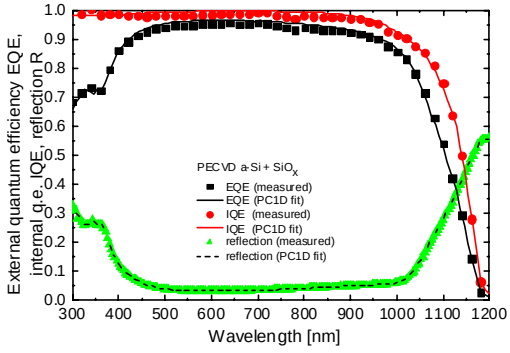

Figure 3: External and internal quantum efficiency and reflection including a PC1D fit for a LFC-PERC cell applying an a-Si + SiO_x rear passivation.

4 a-SiN_x:H + a-SiO_x:H REAR PASSIVATION

In many laboratories, SiN_x layers are a standard means to passivate silicon wafer surfaces for material characterisation due to the excellent surface passivation quality which can be achieved. The passivation mechanism itself typically consists of two elements, a

reduction of the interface state density D_{it} and a field effect induced by fixed, mostly positive, charges within the SiN_x. If a SiN_x is applied as rear passivation in p-type LFC-PERC cells one typically finds a limited rear passivation level which is worse than the surface recombination velocity measured on dedicated lifetime samples. This is typically due to the creation of an inversion layer on the rear and a shunting of this layer by the local rear contacts [10].

This effect can also be found for stacks of SiN_x and SiO_x. In IQE curves this gets clearer. See Figure 5.

However, decent cells of 20.6% efficiency (V_{OC}=670 mV, J_{SC}=38.5 mA/cm^2, FF=79.8%) were reached. The depositions of the SiN_x and the SiO_x were performed in the same plasma tool as the a-Si + SiO_x stacks.

5 a-SiO_x:H + a-SiN_x:H + OPTINALLY a-SiO_x:H REAR PASSIVATION

Since the rather low thermal stability of a-Si rear passivation [7] is a problem in the industrialisation of this approach, an alternative passivation layer system is interesting. Agostinelli et al. have shown that a firing stable surface passivation is possible using a stack of SiO_x and SiN_x layers (with the SiO_x being deposited first) [11]. Somewhat similar stacks and triple stacks of SiO_x, SiN_x and SiO_x (PECVD-ONO) were applied for rear passivation on cell structures as displayed in Figure 2 [12, 13]. Both approaches showed a stability of the passivation effect through the firing. The triple stack ended up in solar cells with the following parameters: η=20.0%, V_{OC}=664 mV, J_{SC}=38.2 mA/cm^2 and FF=78.7%. When applying the same modelling of the rear passivation as shown in section 3, one can extract S_{pass}=500 cm/s ± 50 cm/s for PECVD-ONO on cell level.

The deposition of the thin layers was again performed in the same single-wafer system as above.

6 a-SiC_x:H REAR PASSIVATION

SiC_x layers as well were used for the passivation of the rear of LFC-PERC-type solar cells. SiC_x layers with a substantial share of carbon can provide excellent thermal stability. In most cases the passivation quality increases for SiC_x layers with high silicon content. When applying a single-layer SiC_x layer to small high-efficiency LFC-PERC cells, a maximum efficiency of 20.2% was reached showing a V_{OC} of 665 mV, J_{SC} of 37.5 mA/cm^2 and FF of 80.3% [14]. Riegel et al. presented large-area CZ-Si solar cells applying a SiC_x rear passivation and LFC rear contacts reaching an efficiency of 16.9% (V_{OC}=626 mV, J_{SC}=36.0 mA/cm^2, FF=74.8%) [15]. Riegel et al. used a laser-grooved buried contact front structure.

7 COMPARISON AND DISCUSSION

The presentation of the single results in the previous sections showed that a variety of different passivation layers is available and can reach high efficiencies. The cell results are summarised in Table 1. Since most cells are resulting from different cell batches with slightly varying quality of texture, contacts, oxidation and so on, it is not obvious how the performance of the rear passivation was. Therefore, external quantum efficiency and reflection measurements were performed which can be combined to internal quantum efficiency data. Figure 5 combines a wealth of IQE data of different rear passivation approaches. As reference also a thermally oxidised (high-efficiency approach) and a Al-BSF (industry standard) sample is shown. The sample applying the a-Si + SiO_x layer system (IQE_{1040nm}=88%) performs comparable to the high-end reference SiO_2 (IQE_{1040nm}=90%). The firing-stable passivation layer system PECVD-ONO (IQE_{1040nm}=77%) is performing worse than SiO_2 or a-Si + SiO_x but significantly better than the industrial standard Al-BSF (IQE_{1040nm}=63%). The SiC_x layer system reached about the same quantum efficiency than the Al-BSF sample (IQE_{1040nm}=64%). The SiN_x + SiO_x sample (IQE_{1000nm}=64%) performs comparable to Al-BSF and SiC_x, except in the longest-wavelength region (>1060 nm) where better optics (internal rear reflection) lead to a better performance.

Table 1: Solar cell results of the different rear passivation approaches. The rear passivation layer 1 is located directly on the Si wafer rear surface. Rear passivation layer 2 is placed between layer 1 and the Al. For comparison also cell results that were achieved using a different process flow than shown in Figure 1 are shown.

Rear passivation layer 1	Rear passivation layer 2	Substrate	Area	Base resist.	V_{OC}	J_{SC}	FF	η	Reference
			[cm²]	[Ω cm]	[mV]	[mA/cm²]	[%]	[%]	
PECVD a-Si:H	PECVD SiO_x	FZ-Si	4.0	0.5	677	39.5	81.1	21.7	[5, 6]
PECVD SiO_x	PECVD SiN_x + PECVD SiO_x	FZ-Si	4.0	1.0	664	38.2	78.7	20.0	[13]
PECVD SiN_x	PECVD SiOx	FZ-Si	4.0	0.5	670	38.5	79.8	20.6	unpublished
PECVD SiC_x		FZ-Si	4.0	0.5	665	37.5	80.3	20.2	[14]
thermal SiO_2		FZ-Si	4.0	0.5	685	39.7	80.9	22.0	unpublished
Sputtered SiN_x	PECVD SiO_x	FZ-Si	4.0	0.5	669	38.6	79.7	20.6	[16]
for comparison									
PECVD a-Si:H	PECVD SiN_x	FZ-Si	1.0	1.0	670	39.9	76.5	20.5	[4]
full-area Al-BSF		Cz-Si	147.7	~1.5	614	35.6	79.1	17.4	[17]
PECVD SiO_xN_y	PECVD SiNx	Cz-Si	147.7	~1.5	622	36.2	77.9	17.5	[17]
PECVD SiC_x		Cz-Si	12.5x12.5 pssq	unknown	626	36.0	74.8	16.9	[15]

This draws the attention to Figure 4 which shows a compilation of the long-wavelength reflection values of the different approaches. Here, mainly two groups can be sketched: a first group of all samples with at least one layer of SiO_x incorporated reaching reflection values in the range of 50% to 60%. A second group of SiC_x and Al-BSF which show lower reflection values with SiC_x being in between the SiO_x group and Al-BSF. The long-wavelength reflection gives an idea of the internal rear reflection properties. This value is high if the rear surface is relatively flat and a high step in refractive index is implemented (n_{1000nm} (c-Si)≈3.6, n_{1000nm} (SiO_2) ≈1.5).

Lately, two other interesting process options for industrialisation of LFC-PERC-type cells have been presented. The first ("SiNTO") is applying a thin thermally grown silicon dioxide to the rear. During the oxidation process, the SiN_x anti-reflection coating is already present at the front surface and prevents the oxide from growing at the front surface. On top of the SiO_2 layer, a PECVD stack of a SiO_xN_y and a SiN_x layer and screen-printed Al were deposited. Gautero et al. have shown excellent results on large-area samples prepared using industrial equipment [18]. Comparable cells leaving out the thermal oxide were prepared in ref. [17].

The second approach is aiming on the large-scale implementation of a deposition process for aluminium oxide. Kania et al. showed that the deposition of excellently passivating AlO_x layers is possible using a modified microwave PECVD system by Roth&Rau ("SiNA") which (in unmodified state) is in heavy use in industry for the deposition of ARC SiN_x [19]. The authors showed that these layers exhibit negative charges in large amounts and passivation is possible in the same range than atomic-layer-deposited Al_2O_3.

Bias-light dependent IQE measurements were performed for cells with (i) a-Si + SiO_x, (ii) SiN_x + SiO_x and (iii) thermal SiO_2 rear passivated cells. Figure 6 shows the results of the measurements at 0.0, 0.1, 0.25 and 0.5/0.6 suns. The dependence of the cells to the bias-light is expected to be due to the dependence of the passivation to the excess carrier density (injection). a-Si:H + SiO_x is showing the highest performance at low light intensities. For higher intensities, SiO_2 is comparable to a-Si. SiN_x is getting close to the others for higher injection levels. The SiN_x used in these cells is different to the SiN_x applied in the above discussion. This SiN_x + SiO_x passivated cell ended up with 19.3% in efficiency [20].

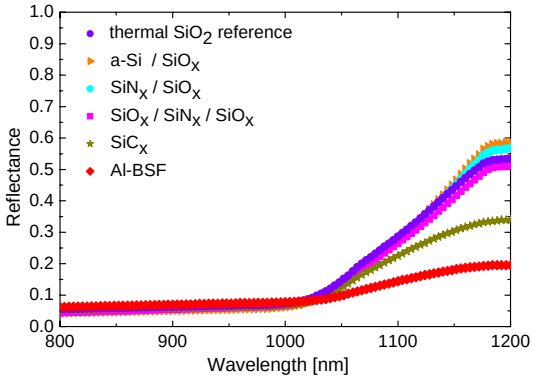

Figure 4: Reflection measurement results of the long-wavelength range of different LFC-PERC-type cells applying a variety of rear surface passivation layer systems. The cells exhibit the structure presented in Figure 2.

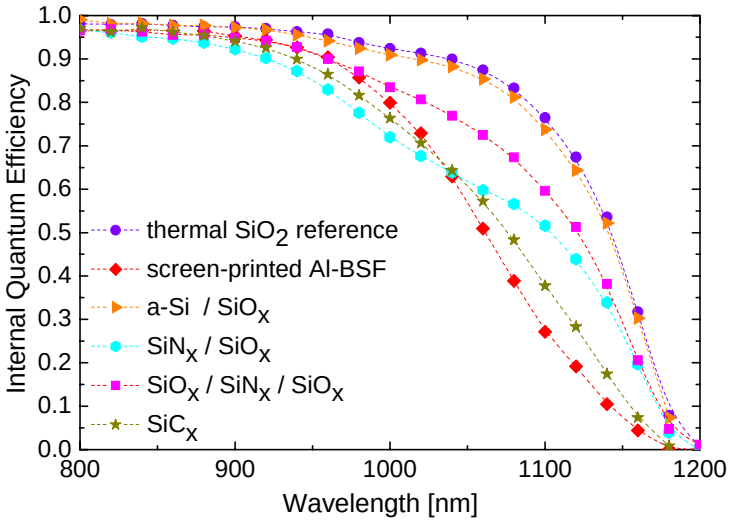

Figure 5: Internal quantum efficiencies for the long-wavelength range of high-efficiency LFC-PERC-type cells applying different rear surface passivation layers. The cells exhibit the structure presented in Figure 2.

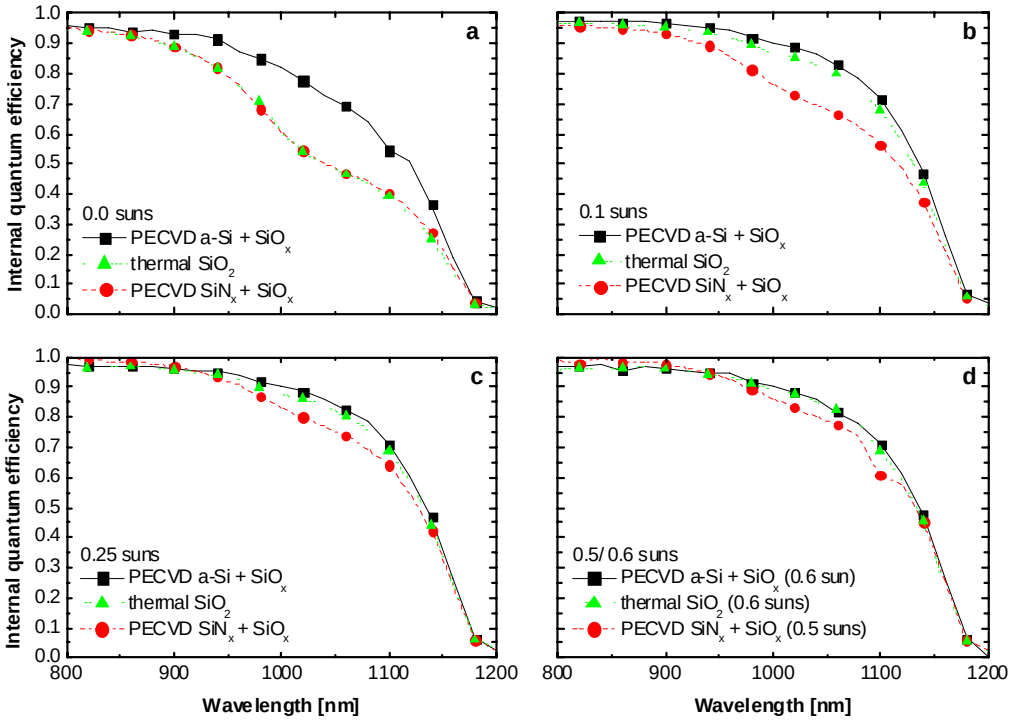

Figure 6: Bias-light-dependent internal quantum efficiency data for high-efficiency LFC-PERC-type cells applying three different rear surface passivation layer systems. The a-Si + SiO_x passivated sample showed the lowest dependence on the bias light, hence the highest injection-independent performance. The SiN_x + SiO_x sample was taken out of a different batch compared to the sample presented above. It showed a lower overall efficiency (η=19.3%) but a better rear passivation in the IQE.

CONCLUSION

The best high-efficiency solar cells produced so far with the different PECVD approaches are summarised here: a-Si:H/SiO_x: η=21.7%, SiC_x: η=20.2%, SiN_x/SiO_x: η=20.6%, SiO_x/SiN_x/SiO_x: η=20.0%, compared to 22.0% of the reference using thermally grown SiO_2.

It can be seen in internal-quantum-efficiency measurements that the a-Si:H approach leads to results comparable to SiO_2. The firing stable stack of SiO_x/SiN_x/SiO_x is found between the highest values of SiO_2 and the lowest values of Al-BSF. SiN_x and SiC_x are ranging at rather low levels.

The measurements of internal rear reflection at long wavelengths show comparable results for SiO_2, SiN_x/SiO_x, SiO_x/SiN_x/SiO_x but lower values for SiC_x.

Simulations of the solar cell behaviour using PC1D [21] and applying the method of Fischer [8] and the results of Kray et al. [9] lead to the conclusion that the rear recombination velocity for the passivated areas is S_{pass}=120 cm/s ± 30 cm/s for the a-Si:H/SiO_x stack and S_{pass}=500 cm/s ± 50 cm/s for PECVD-ONO on cell level.

ACKNOWLEDGEMENT

The authors would like to thank all colleagues at Fraunhofer ISE for their continuous support.

REFERENCES

[1] A.W. Blakers, J. Zhao, A. Wang, A.M. Milne, X. Dai and M.A. Green, Proceedings of the 9th European Photovoltaic Solar Energy Conference, Freiburg, Germany (1989) 328.

[2] E. Schneiderlöchner, R. Preu, R. Lüdemann and S.W. Glunz, Progress in Photovoltaics: Research and Applications 10 (2002) 29.

[3] M. Schaper, J. Schmidt, H. Plagwitz and R. Brendel, Progress in Photovoltaics: Research and Applications 13 (2005) 381.

[4] W. Brendle, V.X. Nguyen, A. Grohe, E. Schneiderlöchner, U. Rau, G. Palfinger and J.H. Werner, Progress in Photovoltaics: Research and Applications 14 (2006) 653.

[5] M. Hofmann, C. Schmidt, N. Kohn, J. Rentsch, S. Glunz and R. Preu, Progress in Photovoltaics: Research and Applications 16 (2008) 509.

[6] M. Hofmann, S. Glunz, R. Preu and G. Willeke, Proceedings of the 21st European Photovoltaic Solar Energy Conference, Dresden, Germany (2006) 609.

[7] M. Hofmann, C. Schmidt, N. Kohn, D. Grambole, J. Rentsch, S.W. Glunz and R. Preu, Proceedings of the 22nd European Photovoltaic Solar Energy Conference Milan, Italy (2007) 1528.

[8] B. Fischer. in Physics, pp. 198, Universität Konstanz, Konstanz 2003.
[9] D. Kray and S.W. Glunz, Progress in Photovoltaics: Research and Applications 14 (2006) 195.
[10] S. Dauwe, L. Mittelstädt, A. Metz and R. Hezel, Progress in Photovoltaics: Research and Applications 10 (2002) 271.
[11] G. Agostinelli, P. Choulat, H.F.W. Dekkers, E. Vermariën and G. Beaucarne, Proceedings of the 4th World Conference on Photovoltaic Energy Conversion, Waikoloa, Hawaii, USA (2006) 1004.
[12] M. Hofmann, S. Kambor, C. Schmidt, D. Grambole, J. Rentsch, S.W. Glunz and R. Preu, Proceedings of the 22nd European Photovoltaic Solar Energy Conference Milan, Italy (2007) 1030.
[13] M. Hofmann, S. Kambor, C. Schmidt, D. Grambole, J. Rentsch, S. Glunz and R. Preu, Advances in OptoElectronics 2008 (2008).
[14] S.W. Glunz, S. Janz, M. Hofmann, T. Roth and G. Willeke, Proceedings of the 4th World Conference on Photovoltaic Energy Conversion, Waikoloa, Hawaii, USA (2006) 1016.
[15] S. Riegel, B. Raabe, R. Petres, S. Dixit, L. Zhou and G. Hahn, Proceedings of the 23rd European Photovoltaic Solar Energy Conference, Valencia, Spain (2008).
[16] W. Wolke. in Fakultät der Mathematik und Physik, pp. 217, Albert-Ludwigs-Universität Freiburg i. Br., Freiburg i. Br. 2005.
[17] M. Hofmann, D. Erath, B. Bitnar, L. Gautero, J.-F. Nekarda, A. Grohe, D. Biro, J. Rentsch and R. Preu, Proceedings of the 23rd European Photovoltaic Solar Energy Conference and Exhibition, Valencia, Spain (2008) 1704.
[18] L. Gautero, M. Hofmann, J. Rentsch, A. Lemke, S. Mack, J. Seiffe, J.-F. Nekarda, D. Biro, A. Wolf, B. Bitnar, et al., Proceedings of the 34th IEEE Photovoltaic Specialist Conference 2009, Philadelphia (2009) in print.
[19] D. Kania, P. Saint-Cast, D. Wagenmann, M. Hofmann, J. Rentsch and R. Preu, this conference, Hamburg (2009).
[20] M. Hofmann, E. Schneiderlöchner, W. Wolke and R. Preu, Proceedings of the 19th European Photovoltaic Solar Energy Conference, Paris, France (2004) 1037.
[21] P.A. Basore, D.T. Rover and A.W. Smith, Proceedings of the 20th IEEE Photovoltaic Specialists Conference, Las Vegas, Nevada, USA (1988) 389.